

## Effect of thermo-mechanical treatment process on microstructure and mechanical properties of 2A97 Al–Li alloy

Chong GAO<sup>1</sup>, Yang LUAN<sup>2</sup>, Jun-chuan YU<sup>1</sup>, Yue MA<sup>1</sup>

1. Key Laboratory of Aerospace Materials and Performance, Ministry of Education, School of Materials Science and Engineering, Beihang University, Beijing 100191, China;
2. College of International Economic and Trade, Liaoning University of International Business and Economics, Dalian 116052, China

Received 17 October 2013; accepted 10 April 2014

**Abstract:** 2A97 Al–Li alloy was processed by thermo-mechanical treatment at different pre-stretch deformations of 0, 3% and 6%. The microstructure observation results reveal that some  $\delta'$  and  $T1$  precipitates are found in  $\alpha(\text{Al})$  matrix of 2A97 alloy processed by the heat treatment with no pre-stretch deformation. When the pre-stretch deformation is 3% and 6%, respectively, amounts of tiny  $T1$  and a few of  $S'$  precipitates are observed in the microstructures of 2A97 alloy. The tensile test results show that the tensile properties of 2A97 alloys are improved via thermo-mechanical treatment. When the pre-stretch deformation is from 0, 3% to 6%, the ultimate tensile strength values of the 2A97 alloys increase gradually from 447.7, 516.5 to 534.3 MPa, and the elongations decrease from 17.6%, 12.8% to 10.2%, respectively. Moreover, with increasing pre-stretch deformation amount from 0 to 6%, the in-plane anisotropy value of 2A97 alloys becomes more obvious.

**Key words:** 2A97 Al–Li alloy; thermo-mechanical treatment; pre-stretch deformation; microstructure; mechanical properties

### 1 Introduction

Aluminum–lithium (Al–Li) alloys are of great interest in structural materials for aerospace applications because of their low density and high strength, good stiffness and reasonable ductility. The marriage of Li to Al offers the promise of substantially reducing the mass of aerospace alloys, since each 1% Li (mass fraction) added to Al reduces the density by 3% and increases the elastic module by about 6% [1,2]. However, due to the anisotropy and poor weld-ability of the alloy, the first and second generations of Al–Li alloy has not been widely used. Until the 1990s, the third generation of Al–Li alloy was developed successfully to have fine comprehensive mechanical properties. In the composition, Li element content reduced and the proportion of Cu increased, which lead to modifying precipitations of  $\delta'$  ( $\text{Al}_3\text{Li}$ , L12 structure),  $\theta$  ( $\text{Al}_2\text{Cu}$ , tetragonal structure) and  $T1$  ( $\text{Al}_2\text{CuLi}$ , hexagonal structure) phases with the processing treatments [3–6].

Heat treatable 2A97 alloy is a new type of Al–Li–Cu alloy, which belongs to the third generation of

Al–Li alloy. There are many researchers concerning the matching of strength and plasticity of 2A97 alloy processed by aging treatment. YUAN et al [7] and LIN et al [8] observed the microstructure of 2A97 alloy under the peak-aged condition. They suggested that the tensile properties of 2A97 alloy were effectively improved by aging treatment, due to a large number of  $T1$  phases precipitated in the matrix. Recently, LI et al [9] reported that the tensile strength of 2A97 alloy aged at 135 °C for 60 h with a pre-deformation amount of 6% was 570 MPa. LIAO et al [10] found that the tensile strength and elongation of the alloy were 605 MPa and 7.7%, respectively under (135 °C, 36 h)+(175 °C, 24 h) duplex aging treatment conditions with 2.5% pre-deformation. These studies suggested that after thermo-mechanical treatment, more and finer  $T1$  precipitates formed in the Al matrix and led to higher tensile strength with favorable plasticity. However, so far, no researches have been published about the anisotropy of 2A97 alloy processed by thermo-mechanical treatment.

In the present study, 2A97 alloy was processed by thermo-mechanical treatment with different pre-stretch deformation amounts of 0, 3% and 6%. The effects of

pre-stretch deformation on the microstructure and mechanical properties of 2A97 alloy were discussed. Moreover, after thermo-mechanical treatment process, the anisotropy of 2A97 alloy was investigated.

## 2 Experimental

The materials used for study were kindly supplied by Aluminum Corporation of China in the form of 4.7 mm-thick hot rolled plate, with a composition of Al base, 4.0% Cu, 1.4% Li (mass fraction used throughout) with minor addition of elements such as 0.4% Mg, 0.5% Zn, 0.3% Mn and 0.1% Zr. The samples of 2A97 alloy were first cold-rolled to sheets with a thickness of 2.2 mm, and then followed by aging treatment at 135 °C for 60 h to reach the peak strength. The processes of 2A97 alloys with different pre-stretch deformations from 0 to 6% are listed in Table 1.

**Table 1** Thermo-mechanical treatment processes of 2A97 alloys

| Alloy    | State                | Solution treatment | Aging treatment |
|----------|----------------------|--------------------|-----------------|
| 2A97-HR  | Hot-rolled           | –                  | –               |
| 2A97-CR  | Cold-rolled          | –                  | –               |
| 2A97-T80 | No pre-stretch+aging | (520 °C, 2 h)      | (135 °C, 60 h)  |
| 2A97-T83 | 3% pre-stretch+aging | (520 °C, 2 h)      | (135 °C, 60 h)  |
| 2A97-T86 | 6% pre-stretch+aging | (520 °C, 2 h)      | (135 °C, 60 h)  |

As an example, three-dimensional micrograph of 2A97-T80 alloy is shown in Fig. 1. The microstructures were characterized by optical microscopy (OM) and transmission electron microscopy (TEM). The hardness measurement was carried out by Vickers micro-hardness tester (HXZ–1000) at a load of 2 N and a dwell time of 10 s. Five measurements were performed to get an average value. The tensile specimens were cut from the alloy sheets by wire electro-discharge machining (EDM), and all the surfaces were mechanically ground with a 600-grit SiC abrasive prior to the tensile test. The tensile

tests were conducted on an Instron–8801 test machine at room temperature and a loading rate of 2 mm/min. The fracture surfaces were observed by a CS–3400 scanning electronic microscope (SEM).

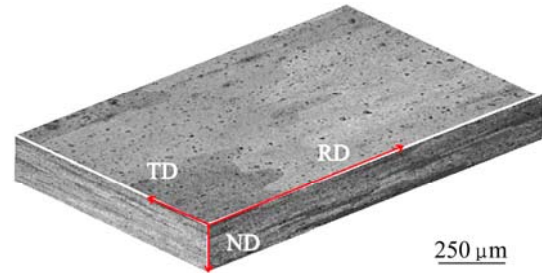


**Fig. 1** Three directions of 2A97-T80 sample (RD—Rolled direction; TD—Transverse direction; ND—Normal direction)

## 3 Results

### 3.1 Tensile properties

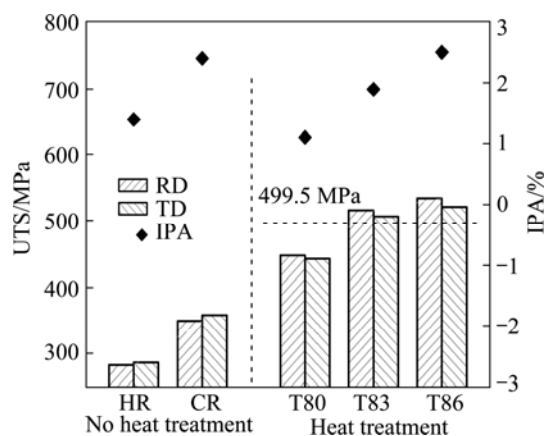
Table 2 shows the tensile properties of 2A97 alloy in 5 different states along rolling direction (RD) and transverse direction (TD). Tensile properties consist of ultimate tensile strength (UTS), yield strength (YS), elongation (EL) and in-plane anisotropy (IPA), which can be calculated in UTS according to Refs. [11,12]

Figure 2 shows UTS and IPA of 2A97 alloys in 5 different states. It reveals that the UTS of 2A97 alloy is greatly enhanced in the heat treatment process. The UTS values of 2A97-HR and 2A97-CR samples are 282.6 and 349.2 MPa, respectively, while the average UTS value of 2A97 alloy processed by heat treatment is 499.5 MPa, which is approximately 2 times of that of 2A97-HR alloy. The scatter diagram of IPA in Fig. 2 indicates that the greater in-plane anisotropy values are directly caused by cold-rolled and pre-stretch deformation. The IPA value of 2A97 alloy processed by cold-rolling is 2.4%, while the IPA value of 2A97-HR alloy is only 1.4%; when the pre-stretch deformation amounts are from 0, 3% to 6%, the IPA values increase from 1.1%, 1.9% to 2.5%.

Figure 3 shows the relationship between the tensile properties of 2A97 alloys processed by heat treatment and the pre-stretch deformation amount. It reveals that the mechanical properties of 2A97 alloy are significantly

**Table 2** Tensile properties of 2A97 alloys along RD and TD directions

| Alloy    | State                | RD-direction |        |      | TD-direction |        |      | IPA(UTS)/% |
|----------|----------------------|--------------|--------|------|--------------|--------|------|------------|
|          |                      | UTS/MPa      | YS/MPa | EL/% | UTS/MPa      | YS/MPa | EL/% |            |
| 2A97-HR  | Hot-rolled           | 282.6        | 261.8  | 18.2 | 286.2        | 262.6  | 15.8 | 1.4        |
| 2A97-CR  | Cold-rolled          | 349.2        | 331.7  | 9.1  | 357.7        | 338.2  | 7.2  | 2.4        |
| 2A97-T80 | No pre-stretch+aging | 447.7        | 411.7  | 17.6 | 442.8        | 389.5  | 11.8 | 1.1        |
| 2A97-T83 | 3% pre-stretch+aging | 516.5        | 499.4  | 12.8 | 506.7        | 470.1  | 7.4  | 1.9        |
| 2A97-T86 | 6% pre-stretch+aging | 534.3        | 516.8  | 10.2 | 521.1        | 501.5  | 7.8  | 2.5        |



**Fig. 2** UTS and in-plane anisotropy (IPA) of 2A97 alloy in five different states

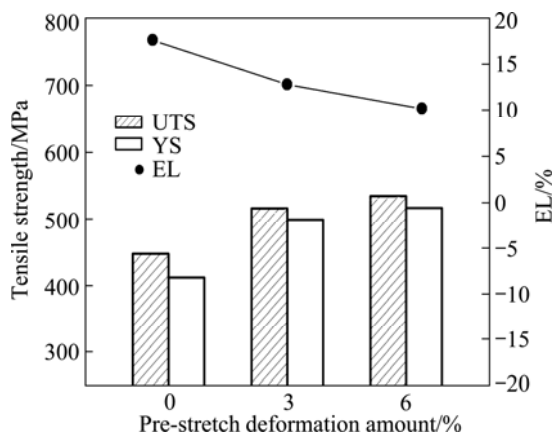


**Fig. 3** Tensile properties of 2A97 alloys processed by heat treatment at different pre-stretch deformation amounts

improved with increasing the pre-stretch deformation amount. When the pre-stretch deformation amount is 0, the UTS, YS and EL of 2A97-T80 alloy are 447.7MPa, 411.7 MPa and 17.6%, respectively; when the pre-stretch deformation amounts are 3% and 6%, the UTS values of 2A97-T83 and 2A97-T86 alloy increase to 516.5 and 534.3 MPa, respectively, while the elongations decrease from 12.8% to 10.2% accordingly.

### 3.2 Hardness

Figure 4 shows the effect of pre-stretch deformation amount on the microhardness of 2A97 alloy. It can be seen from Fig. 4 that the microhardness of 2A97 alloy increases gradually under higher pre-stretch deformation amount condition. When the pre-stretch deformation amounts are 0, 3% and 6%, the microhardness values of 2A97 alloy are HV 165, HV 179 and HV 188, respectively.

### 3.3 Microstructure

Figure 5 shows the micrographs of the hot-rolled 2A97 alloy. It can be seen from Fig. 5(a) that there are

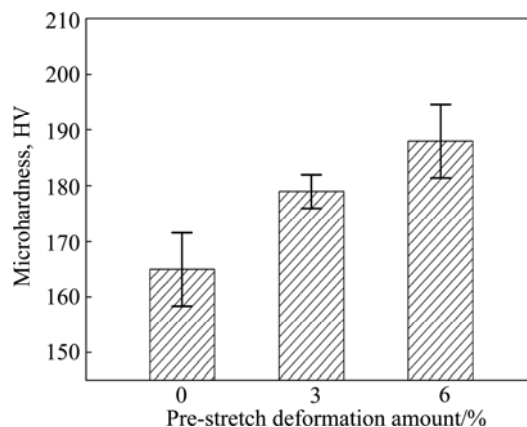


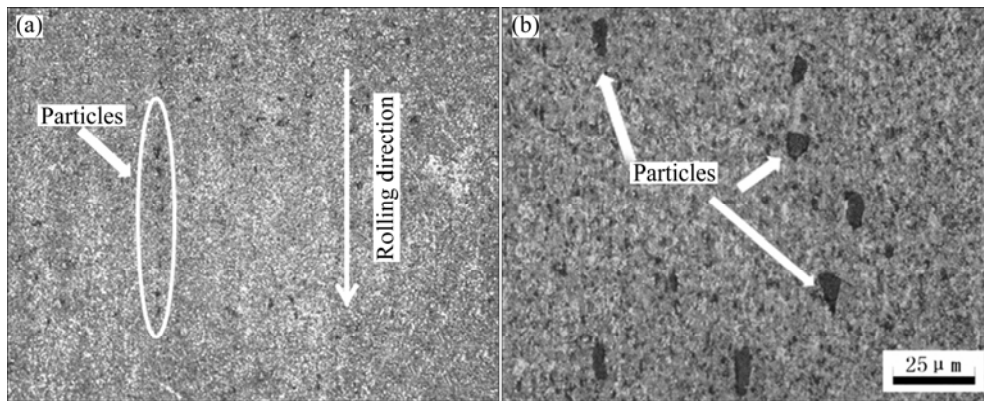
**Fig. 4** Microhardness of 2A97 alloys processed by heat treatment at different pre-stretch deformation amounts

some black particles aligned in the rolling direction in 2A97-HR alloy. A partial magnified micrograph (Fig. 5(b)) reveals that the size of the particles varies from a few micrometers to more than 20  $\mu\text{m}$ . Similar particles were observed in the work of CAMPESTRINI et al [13] and MA et al [14].

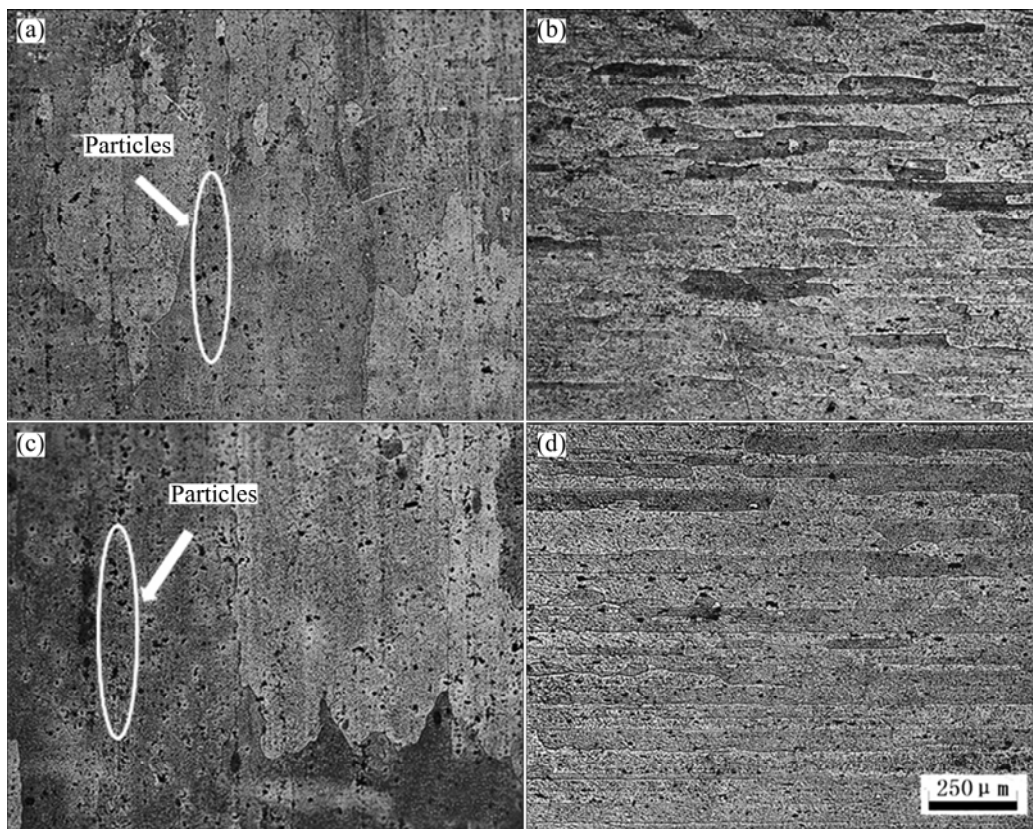
The microstructures of 2A97 alloy under different heat treatment with pre-stretch deformation amounts of 0 and 6% are given in Fig. 6. It can be seen from Figs. 6(a) and (b) that the 2A97-T80 alloy has a “pan-caked” grain structure. The length of the grain is 250–500  $\mu\text{m}$ , and the thickness is 20–40  $\mu\text{m}$ . Figures 6(c) and (d) show that the black particles in 2A97-T80 and 2A97-T86 alloys have no obvious change. And the length of the grain is more than 500  $\mu\text{m}$ , while the thickness remains the same size in 2A97-T86 alloy. The results of tensile tests show that the IPA of the 2A97-T86 alloy is larger than that of the 2A97-T80 alloy. Thus, the elongated grains may have some contribution to the anisotropy.

Figure 7 shows the TEM morphology and SAED pattern of 2A97-HR alloy along the  $[111]_{\text{Al}}$  axis. From Fig. 7, polygonal substructures and no precipitates are observed in 2A97-HR alloy, which indicates that the dynamic recovery plays a dominant role during the hot rolling, and the alloying elements dissolve in the matrix. Thus, the tensile strength of the 2A97-HR alloy is very low.

Figure 8 shows the TEM morphologies of 2A97 alloys with various pre-stretch deformation amount along the  $[\bar{1}12]_{\text{Al}}$  axis. It can be seen from Fig. 8(a) that there are three sets of diffraction spots in the SAED pattern, including aluminum matrix diffraction spots. The super lattice spots (diamond) are from the  $\delta'$  ( $\text{Al}_3\text{Li}$ ) phase (structure: cubic,  $a=0.401$  nm; space group:  $pm\bar{3}m$ ; orientation relationship:  $(100)_{\delta'}/(100)_{\text{Al}}$ ,  $[100]_{\delta'}/(100)_{\text{Al}}$  [14,15]) in the  $[\bar{1}12]$  projection. The diffraction spots at  $1/3 [01\bar{1}]_{\text{Al}}$  (red circles) are from  $T1$  ( $\text{Al}_2\text{CuLi}$ ) phase (structure: hexagonal,  $a=0.496$  nm,  $c=0.935$  nm;



**Fig. 5** Micrographs of hot-rolled 2A97 alloy: (a) Lower magnification; (b) Higher magnification



**Fig. 6** Microstructures of 2A97 alloys under different heat treatment with different pre-stretch deformation amounts: (a) ND plane of 2A97-T80; (b) TD plane of 2A97-T80 alloy; (c) ND plane of 2A97-T86 alloy; (d) TD plane of 2A97-T86 alloy

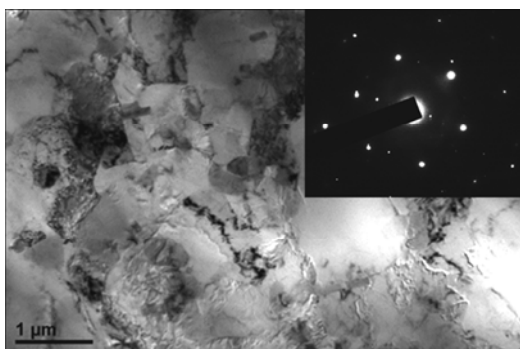


**Fig. 7** TEM morphology and SAED pattern of 2A97-HR alloy along  $[111]_{Al}$  axis

space group:  $P6/mmm$ ; orientation relationship:  $(0001)_{T1} // (111)_{Al}$ ,  $[10\bar{1}0]_{T1} // [1\bar{1}0]_{Al}$ ; habit plane:  $\{111\} [16-18]$  in the  $[\bar{2}110]$  projection. The length of the needle-like  $T1$  precipitates  $\{111\}$  planes is 150–200 nm. Dark shadows are observed around these precipitates, suggesting the presence of a strain field. Spherical  $\delta'$  phases with a diameter of approximately 25 nm are indicated by the arrows. The morphologies of 2A97-T83 and 2A97-T86 alloys are given in Figs. 8(b) and (c), respectively. Amounts of tiny  $T1$  precipitates are found in the length of 80–100 nm in 2A97-T83 alloy, and 50–90 nm in 2A97-T86 alloy, while some  $S'(Al_2CuMg)$

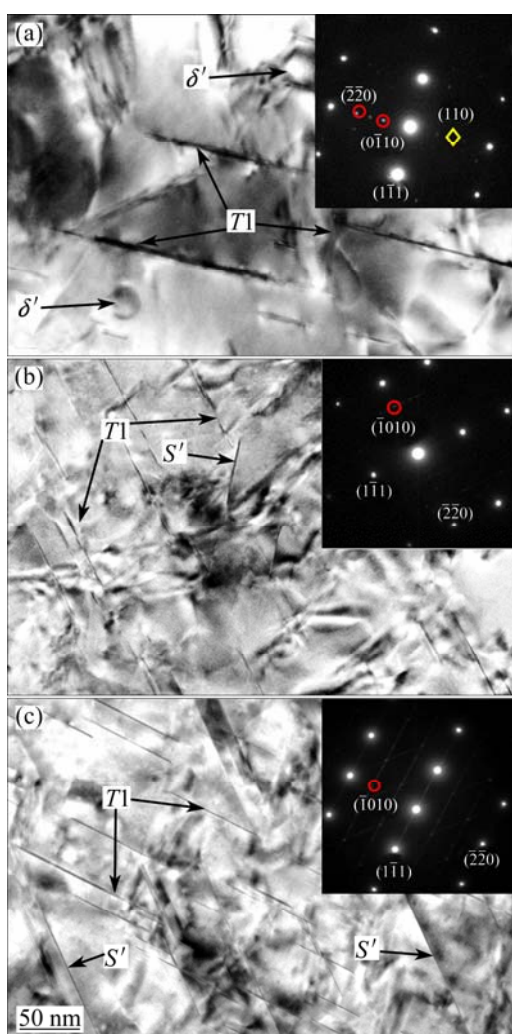


**Fig. 8** TEM morphologies and SAED patterns of 2A97 alloys with various pre-stretch deformation amount along  $[\bar{1}12]_{Al}$  axis: (a) 0%; (b) 3%; (c) 6%

phases are observed.

Here, the underlying mechanism responsible for the improved tensile properties for 2A97 alloys processed by heat treatment was discussed with pre-stretch deformation. GAYLE et al [19] and CASSADA et al [20] indicated that, the  $T1$  precipitates which form in the aluminium  $\{111\}$  planes are considered to have the major strengthening effect in Al–Li alloys. The nucleation of  $T1$  precipitates strongly depends on the application of plastic deformation prior to aging, involving the dissociation of a perfect matrix dislocation. NIE and MUDDLE [21] reported that the strengthening effect produced by  $\{111\}$   $\alpha$  planes (like  $T1$ ) is larger than that produced by  $\{100\}$   $\alpha$  planes and the best strengthening effect is associated with a continuous, three-dimensional network of dispersive, plate-shaped precipitates, similar to those shown in Fig. 8. So, in this work, the mechanical properties of 2A97 alloy are

significantly improved with increasing pre-stretch deformation amount. And the most prominent enhancement of tensile strength happens in the 2A97-T86 alloy with pre-stretch deformation amount of 6%. This is good corresponding to the largest number and fine morphology of  $T1$  precipitates in 2A97 alloys.

MUDDLE and NIE [22] concluded that the nucleation of strengthening precipitates in aluminum based solid solutions is usually heterogeneous, and the heterogeneous nucleation is mostly associated with pre-existing structural defects such as dislocations, stacking faults and grain boundaries so as to reduce the obvious increase of interfacial or strain energies arising from the formation of nuclei. WEI et al [11] believed that the distribution of tiny  $T1$  precipitate phase in  $\alpha(Al)$  matrix may be not uniform.  $T1$  phase precipitates on four  $\{111\}$  planes, and the plane under high shear stress during the pre-stretch deformation has more nucleation sites. The morphologies of Fig. 8 show that the distribution of  $T1$  phase is non-uniform, which is well underpinning the above points of view.

Figure 9 shows the fracture surface morphology of the hot-rolled 2A97 alloy. It reveals that the fracture surfaces are mostly covered with small shallow dimples, and the particles indicated by the arrow fallout from the Al matrix. The fracture mode of 2A97-HR alloy is a quasi-cleavage fracture. Thus, 2A97-HR alloy exhibits good performance in ductility during the tensile test.

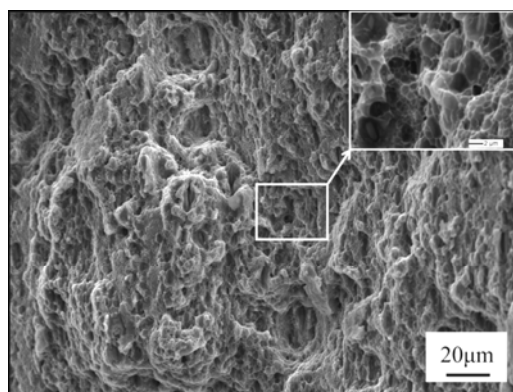


**Fig. 9** Fracture surface morphology of hot-rolled 2A97-HR alloys

Figure 10 shows the fracture surface morphologies of 2A97 alloys with different pre-stretch deformation amounts. From Fig. 10, it can be seen that, the cracks are located at the grain boundaries, lots of small dimples covered on the fracture surfaces, and some particles fallout from the Al matrix. The fracture of 2A97 alloy processed by heat treatment is dominated by the inter-granular mode, which mixes with trans-granular shear mode to some extent.

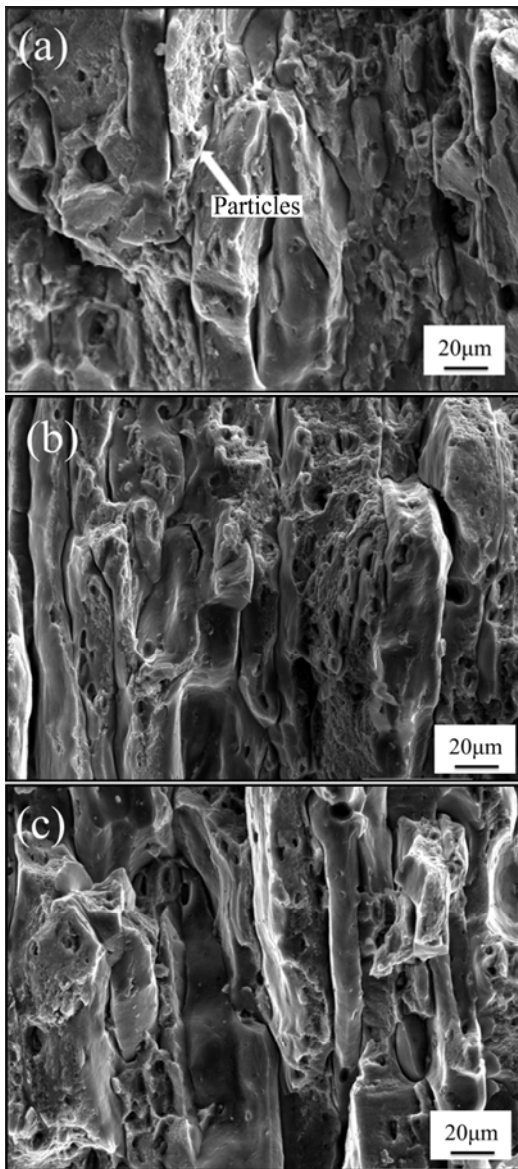


Fig. 10 Fracture surface morphologies of 2A97 alloys with various pre-stretch deformation: (a) 0; (b) 3%; (c) 6%

## 4 Conclusions

1) Tensile properties of 2A97 alloys processed by thermo-mechanical treatment are improved. The UTS values of the 2A97 alloys with pre-stretch deformation amount from 0, 3% to 6% increase gradually from 447.7, 516.5 to 534.3 MPa, and the elongations decrease from 17.6%, 12.8% to 10.2%, respectively.

2) The in-plane anisotropy (IPA) of the 2A97 alloy processed by cold rolling has a greater value of 2.4%, which can be decreased to 1.1% by heat treatment without pre-stretch deformation. When the pre-stretch deformation amounts are 3% and 6%, the IPAs of the heat-treated 2A97 alloy are 1.9% and 2.5%, respectively.

3) The size of  $T1$  precipitates is refined and the precipitation of  $T1$  phase is promoted in 2A97 alloy

processed by heat treatment with pre-stretch deformation amounts of 3% and 6%.

4) The dominant fracture mode of 2A97 alloys processed by thermo-mechanical treatment is the inter-granular rupture.

## References

- [1] ZHENG Zi-qiao, LI Jin-feng, CHEN Zhi-guo, LI Hong-ying, LI Shi-chen, TAN Cheng-yu. Alloying and microstructural evolution of Al–Li alloys [J]. The Chinese Journal of Nonferrous Metals, 2011, 21(10): 2337–2351. (in Chinese)
- [2] LI Jin-feng, ZHENG Zi-qiao, REN Wen-da, CHEN Wen-jing, ZHAO Xu-shui, LI Shi-cha. Simulation on function mechanism of  $T1(Al_2CuLi)$  precipitate in localized corrosion of Al–Cu–Li alloys [J]. Transactions of Nonferrous Metals Society of China, 2006, 16(6): 1268–1273.
- [3] AN L H, CAI Y, LIU W, YUAN S J, ZHU S Q, MENG F C. Effect of pre-deformation on microstructure and mechanical properties of 2219 aluminum alloy sheet by thermomechanical treatment [J]. Transactions of Nonferrous Metals Society of China, 2012, 22(S): s370–s375.
- [4] LEE S, HORITA Z, HIROSAWA S, MATSUDA K. Age-hardening of an Al–Li–Cu–Mg alloy (2091) processed by high-pressure torsion [J]. Materials Science and Engineering A, 2012, 546: 82–89.
- [5] JIANG N, GAO X, ZHENG Z Q. Microstructure evolution of aluminum-lithium alloy 2195 undergoing commercial production [J]. Transactions of Nonferrous Metals Society of China, 2010, 20(3): 740–745.
- [6] RANGANATHA R, KUMAR ANIL V, NANDI VAISHAKI S, BHAT R R, MURALIDHARA B K. Multi-stage heat treatment of aluminum alloy AA7049 [J]. Transactions of Nonferrous Metals Society of China, 2013, 23: 1570–1575.
- [7] YUAN Z S, LU Z, XIE Y H, DAI S L, LIU C S. Effect of plastic deformation on microstructure and properties of high strength Al–Cu–Li–X aluminum-lithium alloy [J]. Rare Metal Materials and Engineering, 2007, 36(3): 493–496. (in Chinese)
- [8] LIN Yi, ZHENG Zi-qiao, ZHANG Hai-feng, HAN Ye. Effect of heat treatment process on tensile properties of 2A97 Al–Li alloy: Experiment and BP neural network simulation [J]. Transactions of Nonferrous Metals Society of China, 2013, 23(6): 1728–1736.
- [9] LI Hong-ying, WANG Xiao-feng, BIN Jie, WEI Dong-dong, ZHANG Jian-fei. Effect of two aging processes on microstructure and properties of alloy 2A97 [J]. Journal of Central South University: Science and Technology, 2011, 42(5): 1261–1269. (in Chinese)
- [10] LIAO Z Q, ZHENG Z Q, ZHONG S, CAI B, LI S C. Effect of ageing treatment on local corrosion behavior and microstructure of 2A97 Al–Li alloy [J]. Materials Science and Engineering of Powder Metallurgy, 2011(4): 478–486. (in Chinese)
- [11] WEI Q L, CHEN Z, WANG Y X. Contribution of  $T1$  precipitate ( $Al_2CuLi$ ) to anisotropy in Al–Li alloys [J]. Nonferrous Metal, 2002(3): 4–8. (in Chinese)
- [12] JATA K V, HOPKINS A K, RIOJA R J. The anisotropy and texture of Al–Li alloys [J]. Mat Sci Forum, 1996, 647: 217–222.
- [13] CAMPESTRINI P, van WESTING E P M, van ROOIJEN H W, de WIT J H W. Relation between microstructural aspects of AA2024 and its corrosion behavior investigated using AFM scanning potential technique [J]. Corrosion Science, 2000, 42(11): 1853–1861.
- [14] MA Y, ZHOU X, THOMPSON G E, HASHIMOTO T, THOMSON P, FOWLES M. Distribution of intermetallics in an AA 2099-T8 aluminium alloy extrusion [J]. Materials Chemistry and Physics, 2011, 126(1–2): 46–53.

- [15] WANG S, STARINK M. Precipitates and intermetallic phases in precipitation hardening Al–Cu–Mg–(Li) based alloys [J]. *International Materials Reviews*, 2005, 50(4): 193–215.
- [16] YOSHIMURA R, KONNO T J, ABE E, HIRAGA K. Transmission electron microscopy study of the early stage of precipitates in aged Al–Li–Cu alloys [J]. *Acta Materialia*, 2003, 51: 2891–2903.
- [17] DONNADIEU P, SHAO Y, de GEUSER F, BOTTON G A, LAZAR S, CHEYNET M. Atomic structure of  $T_1$  precipitates in Al–Li–Cu alloys revisited with HAADF-STEM imaging and small-angle X-ray scattering [J]. *Acta Materialia*, 2011, 59: 462–72.
- [18] MUÑOZ-MORRIS M, MORRIS D. Severe plastic deformation processing of Al–Cu–Li alloy for enhancing strength while maintaining ductility [J]. *Scripta Materialia*, 2010, 63(3): 304–307.
- [19] GAYLE F W, HEUBAUM F H, PICKENS J R. Structure and properties during aging of an ultra-high strength Al–Cu–Li–Ag–Mg alloy [J]. *Scripta Metallurgica et Materialia*, 1990, 24(1): 79–84.
- [20] CASSADA W, SHIFLET G, STARKE E. The effect of plastic deformation on  $Al_2CuLi$  ( $T_1$ ) precipitation [J]. *Metallurgical Transactions A*, 1991, 22(2): 299–306.
- [21] NIE J F, MUDDLE B C. Microstructural design of high-strength aluminum alloys [J]. *Journal of Phase Equilibria*, 1998, 19(6): 543–551.
- [22] MUDDLE B C, NIE J F. Nucleation-mediated structural refinement and aluminium alloy design [J]. *Materials Science Forum*, 2006, 519–521: 191–196.

## 形变热处理工艺对铝锂合金 2A97 显微组织和力学性能的影响

高崇<sup>1</sup>, 栾阳<sup>2</sup>, 于俊川<sup>1</sup>, 马岳<sup>1</sup>

1. 北京航空航天大学 材料科学与工程学院 航空航天材料和性能教育部重点实验室, 北京 100191;
2. 辽宁对外经贸学院 国际经济贸易学院, 大连 116052

**摘要:** 采用不同(0、3%和 6%)的预拉伸变形的形变热处理强化工艺处理 2A97 铝锂合金。显微组织研究结果表明, 在无预拉伸变形的热处理 2A97 合金中发现了  $\delta'$  和  $T_1$  两种强化相; 当预变形量为 3%和 6%时, 大量细小的  $T_1$  相析出, 且低观察到少量  $S'$ 相。拉伸测试结果表明, 变形热处理对 2A97 合金的拉伸性能具有显著影响, 且随着预拉伸变形量由 0、3%变化到 6%, 合金的抗拉强度分别由 447.7、516.5 提高到 534.3 MPa, 而伸长率相应地由 17.6%、12.8% 降低到 10.2%。此外, 随着预拉伸变形由 0 增加到 6%, 2A97 合金的各向异性更显著。

**关键词:** 2A97 铝锂合金; 形变热处理; 预拉伸变形; 显微组织; 力学性能

(Edited by Wei-ping CHEN)